Distance between homologous chromosomes results from chromosome positioning constraints

Claire Heride[1,*], Michelle Ricoul[1], Kien Kiêu[2], Johann von Hase[3], Vincent Guillemot[4], Christoph Cremer[3], Karine Dubrana[1,‡,§] and Laure Sabatier[1,‡,§]

[1]Laboratoire de Radiobiologie et d'Oncologie (LRO), Commissariat à l'Energie Atomique, 92 265 Fontenay-aux-Roses Cedex, France
[2]UR 341 Mathématiques et Informatique Appliquées, INRA, 78 350 Jouy-en-Josas, France
[3]Kirchhoff Institute for Physics, University of Heidelberg, 69 120 Heidelberg, Germany
[4]Laboratoire d'Exploration Fonctionnelle des Génomes (LEFG), Commissariat à l'Energie Atomique, 91 057 Evry, France
*Present address: Physiological Laboratory, School of Biomedical Sciences, University of Liverpool, Liverpool L69 3BX, UK
‡These authors contributed equally to this work
§Authors for correspondence (karine.dubrana@cea.fr; laure.sabatier@cea.fr)

Accepted 9 August 2010
Journal of Cell Science 123, 4063-4075

doi:10.1242/jcs.066498

Summary

The organization of chromosomes is important for various biological processes and is involved in the formation of rearrangements often observed in cancer. In mammals, chromosomes are organized in territories that are radially positioned in the nucleus. However, it remains unclear whether chromosomes are organized relative to each other. Here, we examine the nuclear arrangement of 10 chromosomes in human epithelial cancer cells by three-dimensional FISH analysis. We show that their radial position correlates with the ratio of their gene density to chromosome size. We also observe that inter-homologue distances are generally larger than inter-heterologue distances. Using numerical simulations taking radial position constraints into account, we demonstrate that, for some chromosomes, radial position is enough to justify the inter-homologue distance, whereas for others additional constraints are involved. Among these constraints, we propose that nucleolar organizer regions participate in the internal positioning of the acrocentric chromosome HSA21, possibly through interactions with nucleoli. Maintaining distance between homologous chromosomes in human cells could participate in regulating genome stability and gene expression, both mechanisms that are key players in tumorigenesis.

Key words: Chromosome territory, Nuclear organization, Homologues, Heterologues, Nucleolar organizer region, Human

Introduction

The nucleus is a highly compartmentalized organelle with specialized domains that perform distinct functions, such as transcription, RNA processing and replication (for reviews, see Cremer and Cremer, 2001; Gilbert et al., 2005; Rouquette et al., 2010). In most higher eukaryotes, individual chromosomes are not spread out throughout the nucleus but occupy distinct and defined territories (for a review, see Cremer et al., 1993). Although there is no evidence of a particular positioning of chromosome territories (CTs) relative to each other, they are not randomly organized in the nuclear space (Bolzer et al., 2005; Cornforth et al., 2002; Kozubek et al., 2002). A radial organization has been observed in many eukaryotic cells, such as human, mouse, chicken and plants, and throughout species of the primate phylum, with some chromosomes preferentially located towards the center of the nucleus, whereas others are more peripheral (Croft et al., 1999; Habermann et al., 2001; Mayer et al., 2005; Mora et al., 2006; Nagele et al., 1999; Neusser et al., 2007; Parada and Misteli, 2002; Tanabe et al., 2005; Tanabe et al., 2002). Such a conservation through evolution suggests a strong functional significance of this nuclear architecture.

Despite the apparent importance of intranuclear chromosome positioning, little is known about the underlying mechanisms. It has been observed that gene-rich chromosomes are located preferentially at the center of the nucleus, whereas gene-poor chromosomes are found closer to the periphery (Boyle et al., 2001; Bridger et al., 2000; Cremer et al., 2003; Cremer et al., 2001; Croft et al., 1999), an arrangement that correlates with the transcriptional activity of chromosomes (Kozubek et al., 2002). Others have described a correlation between the size of the chromosomes and their radial nuclear position, in which large chromosomes are statistically more peripheral than smaller ones (Bolzer et al., 2005; Bridger et al., 2000; Cremer et al., 2001; Mora et al., 2006; Sun et al., 2000). The significance of such correlations is still a matter of debate.

A way to constrain chromosome positioning is to anchor specific chromosomal structures to nuclear components. This has been shown in the budding yeast *Saccharomyces cerevisiae*, where centromeres cluster at one side of the nucleus through interaction with the spindle pole body (Bystricky et al., 2004; Guacci et al., 1997; Heun et al., 2001; Jin et al., 1998), whereas telomeric peripheral foci are anchored to the nuclear envelope (Gotta and Gasser, 1996), leading to a Rabl-like organization (Bystricky et al., 2005). In mammals, nuclear matrix components and the nuclear envelope also appear to be potential anchors for chromosome territories. Indeed, in human cells, a genome-wide mapping of lamin B1 binding sites has recently shown that this protein is not evenly bound to all chromosomes and that the number of lamin B1 interactions per chromosome correlates with their radial positioning (Guelen et al., 2008). Moreover, recent studies have shown that modifications of the expression of lamina proteins influence the radial positioning of some peripheral chromosomes (Malhas et al., 2007; Meaburn et al., 2007). Finally, the tethering of the inner nuclear membrane protein Lap2β to a chromosomal locus is sufficient to reposition the entire chromosome territory at the nuclear periphery (Finlan et al., 2008), showing that a single anchoring site is enough to determine the radial position of a

whole chromosome. The nuclear envelope and the associated nuclear matrix proteins then appear to be involved in the peripheral targeting of chromosomes. However, it remains unclear whether the internal positioning of CTs is the default state or results from an active anchoring to internal nuclear structures.

The radial organization of chromosomes, with particular chromosomes tending to be at the nuclear interior and others at the periphery, might per se give rise to preferred neighboring of chromosomes. However, the measurements of angles between CTs or between different loci have shown that most human chromosomes have no specific neighbors (Bolzer et al., 2005; Cornforth et al., 2002; Kozubek et al., 2002). These results do not preclude there being more subtle rules for the organization of chromosomes relative to each other, but a simple general arrangement failed to emerge. This is probably due to the variable nature of chromosome positioning and to cell cycle, cell type, or tissue specificity (Parada et al., 2004). Several studies have shown that some chromosomes are preferentially closer to each other than expected if they were randomly arranged in the nucleus (Bolzer et al., 2005; Cremer et al., 2001; Parada et al., 2002). Notably, small gene-rich chromosomes that frequently colocalize at the center of the nucleus in FISH experiments (Boyle et al., 2001; Tanabe et al., 2002) have been shown to preferentially interact with each other by the Hi-C method (Lieberman-Aiden et al., 2009). In addition, homologues of centrally located acrocentric chromosomes that contain nucleolar-organizer regions tend to associate with each other, possibly as a consequence of their interaction with nucleoli (Bolzer et al., 2005; Chandley et al., 1996). However, the mean distances observed between acrocentric chromosomes are not significantly different from the mean distances observed between other small, centrally located chromosomes (Bolzer et al., 2005).

Homologous chromosomes have been shown to exhibit a low frequency of joint damage after laser-uv-microirradiation and caffeine treatment in Chinese hamster lung cells (Cremer et al., 1982) and to rearrange infrequently after irradiation (Boei et al., 2006). This suggests that homologues are generally distant from each other in the nucleus. However, rearrangements between homologous chromosomes are poorly detected, and such an organization needs to be confirmed. Recently, the study of chromosome arrangements in the mouse has shown that chromosome territories tend to adopt a nonrandom position within the nucleus and actually assemble in heterologous neighborhoods (Khalil et al., 2007). Whether this characteristic is conserved in human cells has not been addressed.

Using multicolor 3D-FISH and 3D image analysis to keep the interphase nuclear structure and avoid eventual biases with two-dimensionally projected images, we investigated the distribution of chromosome territories in the nucleus and relative to each other. We show that the radial positioning of chromosome territories in human epithelial bladder cancer cells correlates with the ratio of gene density to chromosome size. To determine the organization of chromosomes relative to each other, we measured the distances between the gravity centers and between the edges of chromosome territories. We observed that a chromosome is generally closer to a heterologue than to its homologue. Using numerical simulations, we demonstrate that, for some chromosomes, a constrained radial position is sufficient to explain the inter-homologue distance, whereas, for others, additional constraints must be involved. We also present experimental data that support the implication of nucleolar organizer region sequences in the internal positioning of the acrocentric chromosome HSA21.

Results

Chromosome territories are radially positioned relative to the ratio of gene density to chromosome size in epithelial cancer cells

Whether the radial organization of chromosomes correlates with gene density or chromosome size, and how these parameters influence intranuclear chromosome positioning is still a matter of debate. Here, we used advanced microscopy and image analysis tools to analyze in three dimensions the radial positions of 10 chromosomes in the EJ-30 epithelial cancer cell line. We visualized single chromosomes by fluorescence in situ hybridization (FISH) using whole-chromosome-specific probes and analyzed their position in interphase cells containing a diploid complement of fluorescent signals. To be able to compare the radial position distribution with various parameters, we chose to examine large (HSA1 and 4), small (HSA18, 19 and 21), gene-rich (HSA17 and 19) and gene-poor chromosomes (HSA4, 8, 18 and 21) and chromosomes that are intermediate for these characteristics (HSA10, 14 and 16) (Table 1). Chromosomes were labeled using a 3D-FISH protocol that has previously been shown to preserve the 3D topology of chromosome territories and chromosomal subregions (Fig. 1) (Solovei et al., 2002). Optical serial sections were recorded on a wide-field microscope and deconvolved before any analysis. After thresholding, each labeled voxel was located in one of 20 concentric 3D nuclear shells, as described previously by Cremer and colleagues (Cremer et al., 2001). As this evaluation

Table 1. Characteristics of the studied chromosomes

HSA	Size (Mb)	Number of genes	Gene density (genes/Mb)	Gene density per size	Median of RRD (%)	Hardcore radii (μm)
1	247	3923	15.9	6.4×10^{-2}	73.6	0.48
4	191	1281	6.7	3.5×10^{-2}	78.9	0.65
8	146	1204	8.2	5.6×10^{-2}	77.1	0.78
10	135	1594	11.8	8.7×10^{-2}	69.6	0.77
14	106	1324	12.5	1.2×10^{-1}	65.4	0.46
16	89	1186	13.3	1.5×10^{-1}	66.8	0.52
17	79	1727	21.9	2.8×10^{-1}	59.1	0.28
18	76	478	6.3	8.3×10^{-2}	68.9	0.43
19	64	1762	27.5	4.3×10^{-1}	51.9	0.56
21	47	456	9.7	2.1×10^{-1}	59.9	0.38

Chromosome size and gene numbers were extracted from the Map Viewer database (http://www.ncbi.nlm.nih.gov/projects/mapview/maps.cgi?TAXID=9606&). The number of genes was sourced from the Ensembl database. The medians of the RRD (relative radial distribution) values were determined, with the cumulative frequency curves representing the relative radial distribution shown in Fig. 2. The hardcore radii were determined from the smallest observed distances between chromosome territories (CTs).

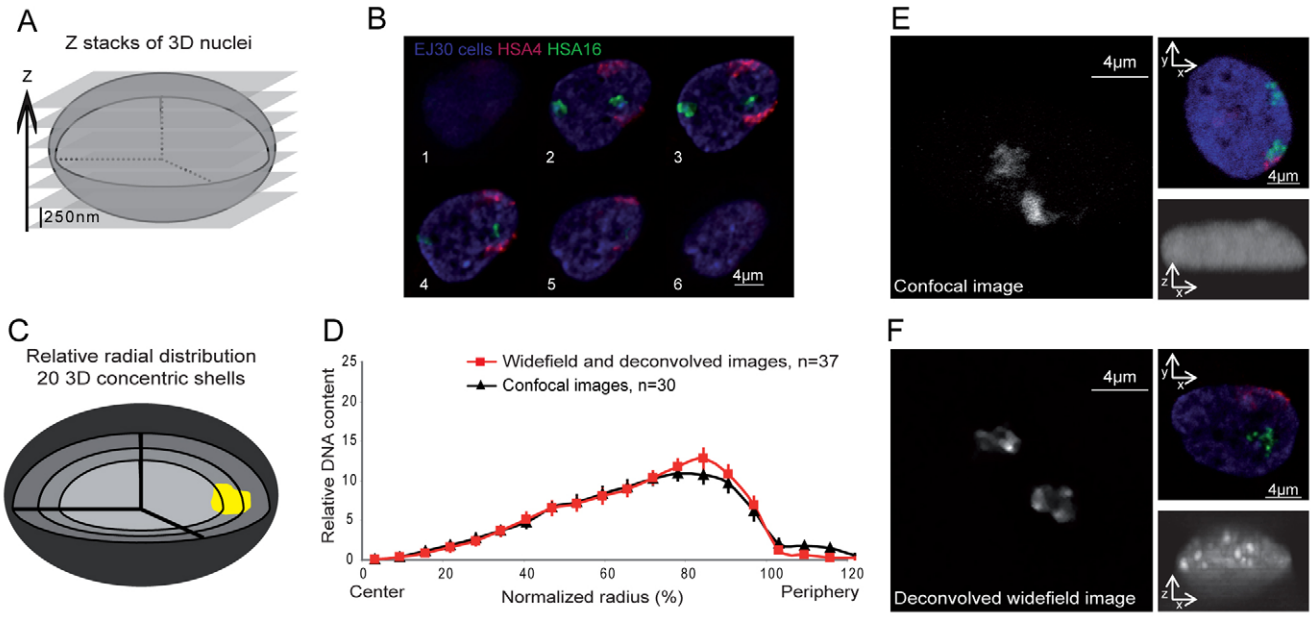

Fig. 1. Comparison of CT radial distributions measured from confocal or wide-field images. (**A**) Images in three dimensions of preserved nuclei were acquired with 250 nm *z*-steps. (**B**) Typical optical sections of a nucleus hybridized with probes for HSA4 (magenta) and HSA16 (green) and counterstained with DAPI (blue). (**C**) Three-dimensional (3D) evaluation of the radial position of chromosome territories. Each nucleus was divided into 20 equidistant shells, and the sum of voxel intensities for each fluorochrome was quantified in each shell. (**D**) The relative radial distribution (RRD) corresponding to the DNA content of chromosome 16 relative to a normalized relative nuclear radius (%) was determined on images acquired either with a confocal microscope (black triangles, n=30) or a wide-field microscope (red squares, n=37) in ClH2 cells. A gray-scale coding of a chromosome territory (CT) FISH image, a focal plan and section of a nucleus acquired with either a confocal microscope (**E**) or a wide-field microscope (**F**) are shown.

method was previously applied only on confocal images, we checked that deconvolved wide-field images were suitable for these measurements by assessing the radial position of HSA16. We observed no statistical difference in the radial position of HSA16 evaluated from wide-field deconvolved images and confocal images (Fig. 1) and thus chose to pursue our analysis on wide-field images, which exhibit a better signal-to-noise ratio. The chromosomes studied here present various radial positions: HSA4, 8 and 1 are the most peripheral; HSA10, 18, 16 and 14 present an intermediate radial position; whereas HSA21, 17 and 19 are internal (Fig. 2). The radial position of chromosome territories in human cells has been proposed to correlate either with chromosome size (Bolzer et al., 2005; Cremer et al., 2001; Sun et al., 2000) or with gene density (Boyle et al., 2001; Bridger et al., 2000; Cremer et al., 2003; Croft et al., 1999). In an attempt to visualize the correlation between radial position and chromosome size or gene density, we classified the analyzed chromosomes into three categories based on decreasing size, increasing gene density, or increasing ratio of gene density to chromosome size and plotted their corresponding radial position profiles (Fig. 2). Although, in some cases, chromosomes of similar size exhibited similar radial positions (HSA14–HSA16; Table 2), there were often cases where similarly sized chromosomes adopted statistically different radial positions (HSA1–HSA4; HSA16–HSA17; HSA17–HSA18; HAS18–HSA19; HSA19–HSA21; Tables 1 and 2; Fig. 2A). In order to quantify the chromosome-size-dependent radial positioning, median radial positions were plotted relative to chromosome size. The linear regression of these data shows a weak but significant correlation between these two parameters (R^2=0.58; P=0.01; Fig. 2D). However, HSA21, the smallest chromosome studied, does not represent the lowest relative radial position. HSA21, one of the acrocentric chromosomes, bears nucleolar organizers, which could impose additional positional constraints. As described previously (Cremer et al., 2003; Croft et al., 1999), HSA18 also escapes this rule as it is more peripheral than expected based on its size. Several previous studies analyzing the relative position of HSA18 and HSA19 have proposed that radial positioning was correlated with gene density (Boyle et al., 2001; Bridger et al., 2000; Cremer et al., 2003; Croft et al., 1999). We observed that chromosomes with similar gene density have statistically different radial positions (HSA4–HSA18; HSA8–HSA21; HSA1–HSA16; Tables 1 and 2; Fig. 2B,E). Linear regression shows a weak, but significant, correlation between median radial positions and gene density (R^2=0.56; P=0.01; Fig. 2E). However, HSA21 is not peripherally located, as expected from its gene density; HSA1 and HSA10 also strongly deviate from the linear regression.

These linear regressions show that there is almost the same correlation between the radial position and chromosome size (R^2=0.58; P=0.01; Fig. 2D) and the radial position and gene density (R^2=0.56; P=0.01; Fig. 2E), suggesting that both size and gene density affect chromosome radial positioning to some extent. In an attempt to define the contribution of these two parameters, we compared the radial position of chromosomes with the ratio of gene density to chromosome size (Fig. 2C,F). The chromosomes HSA10 and HSA18, which have a similar ratio of gene density to chromosome size (8.7×10^{-2} and 8.3×10^{-2}, respectively), share the same radial position. Most chromosomes follow this rule, as a plot of the median radial position against the ratio of gene density to chromosome size reveals a strong correlation (R^2=0.87; P=0.7×10^{-4}; Fig. 2F). The ratio of gene density to chromosome

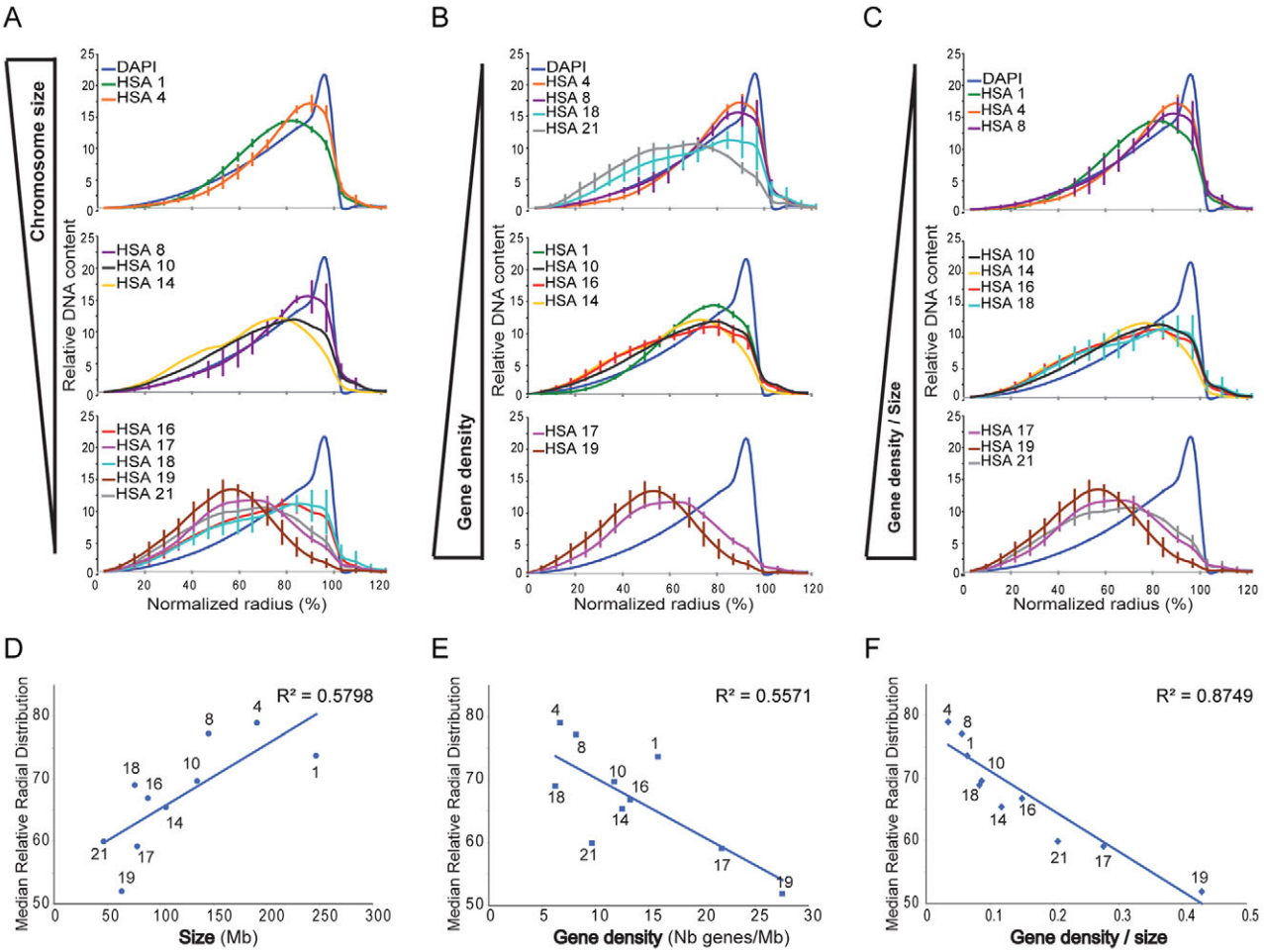

Fig. 2. Chromosome territories are radially positioned relative to their gene density, to their size and to the ratio of gene density to chromosome size. For each vertical panel, the relative radial distributions (RRDs) of the analyzed chromosomes and of the DAPI-counterstained DNA measured in EJ-30 cells were classified according to the chromosome size (**A**), the gene density (**B**) or to the gene density-to-chromosome size ratio (**C**). Depicted are: HSA1 (green, *n*=163), HSA4 (orange, *n*=131), HSA8 (purple, *n*=94), HSA10 (dark gray, *n*=90), HSA14 (yellow, *n*=52), HSA16 (red, *n*=572), HSA17 (pink, *n*=98), HSA18 (turquoise, *n*=187), HSA19 (brown, *n*=194), HSA21 (pale gray, *n*=85) and DAPI (blue, *n*=821) (error bar=s.e.m.). In each case, the linear regression of the specified parameter with the median relative radial distribution is shown (**D–F**). The straight line is the best-fit linear regression line with R^2 (correlation coefficient).

size corresponds to the ratio of the gene number to the square of the chromosome size. This suggests that, in EJ-30 cells, gene number and chromosome size are inversely contributing to the radial positioning of chromosomes, with the size parameter showing a stronger contribution than the gene number.

A chromosome is generally closer to a heterologue than to its homologue

We sought to investigate the spatial relationship between chromosomes in human cancer epithelial cells. Each nucleus was hybridized with probes specific to two different chromosomes, and interchromosomal distances were analyzed by two independent methods: measurements of distances between the gravity centers and measurements of distances between the edges of chromosome territories (Fig. 3A,B). We first checked whether our measurements can discriminate close and distant chromosomes. To this end, we used a subclone (ClH2) isolated from the EJ-30 cell line that contains a single additional translocation involving HSA16 and HSA21, t(16;21) (Fig. 6C,D). In most of the cells, we were able to distinguish a double color signal corresponding to the chromosome translocation t(16;21) as well as additional single signals corresponding to the normal chromosomes HSA16 and HSA21 (Fig. 6F). As expected for two chromosomes in contact, the mean distance measured between the gravity center of the two closest HSA16 and HSA21 chromosomes in ClH2 cells roughly corresponds to the sum of the mean radii of chromosomes HSA16 and HSA21 (data not shown). This distance in ClH2 cells is statistically different from the distance observed in EJ-30 cells (1.63±0.01 μm and 3.20±0.16 μm, respectively; $P=5.21\times10^{-13}$; Fig. 3C), showing that this method enables us to distinguish between close and distant chromosomes.

As an independent and complementary approach, the distances between HSA16 and HSA21 were analyzed by measuring edge-to-edge distances with the ADS program (Khalil et al., 2007; Solovei et al., 2009), which provides the 3D distance between the two closest voxels of two chromosomes. Fig. 3D shows that the distance between the edges of the chromosomes 16 and 21 involved in the translocation is equal to zero, whereas the non-translocated chromosomes in EJ-30 cells are separated by 0.90±0.11 μm. These distances are statistically different ($P=1.31\times10^{-10}$), showing that

Table 2. Statistical difference in relative radial distribution (nonparametric multivariate tests)

HSA	1	4	8	10	14	16	17	18	19
4	1.64×10^{-5}								
8	3.29×10^{-10}	7.98×10^{-3}							
10	5.73×10^{-6}	5.47×10^{-7}	2.37×10^{-3}						
14	2.91×10^{-10}	5.01×10^{-9}	1.84×10^{-4}	3.62×10^{-3}					
16	3.06×10^{-10}	2.67×10^{-16}	0.02	0.14	0.26				
17	0	0	4.89×10^{-13}	4.05×10^{-5}	7.26×10^{-5}	8.91×10^{-11}			
18	0	1.87×10^{-12}	1.38×10^{-4}	0.01	0.12	0.01	6.26×10^{-8}		
19	0	0	0	0	9.31×10^{-12}	0	1.62×10^{-4}	9.99×10^{-14}	
21	0	0	1.01×10^{-10}	1.24×10^{-3}	5.46×10^{-3}	5.95×10^{-3}	3.25×10^{-3}	1.64×10^{-3}	7.96×10^{-11}

For each pair of heterologous chromosomes, nonparametric multivariate tests were applied to compare the relative radial distribution of chromosome territories (CTs). HSA, *Homo sapiens* autosome.

this method allows us to quantify proximities between chromosomes and accurately determine when two chromosomes are in contact.

We first measured the distances between the gravity centers (GC distance) of homologous or heterologous chromosomes in 1200 nuclei hybridized with probes for two chromosomes (Fig. 3E). The percentage of nuclei with inseparable homologues ranged from 8 to 30%, depending on the chromosome studied, the largest values being observed for the most centrally located chromosomes HSA17 and HSA19, which exhibit 18% and 30% of overlapping homologues, respectively (for details, see supplementary material Table S1). These images were, however, taken into account for the estimation of the inter-homologue distances and were counted as exhibiting a GC distance equal to zero. By contrast, when heterologous chromosomes are in contact, the measured GC distance is always positive. Our measurements thus underestimate the inter-homologue distances but do not affect the inter-heterologue distances. Despite this bias, a global analysis showed that the mean distance between two homologous chromosomes is significantly larger (despite being underestimated) than the mean distance between the closest heterologues (4.50±0.05 µm and 3.05±0.04 µm, respectively; P=0; Fig. 3E). To investigate whether this observation holds for different pairs of chromosomes, we compared the inter-homologue and inter-heterologue GC distances of pairs of chromosomes presenting a diverse radial position (Fig. 4; Table 3). The inter-homologue distances measured for the peripheral chromosomes HSA1 and HSA4 were significantly larger than the HSA1–HSA4 inter-heterologue distance (Fig. 4A; Table 3). The same was observed for the inter-homologue distances of chromosomes presenting an intermediate radial position (HSA10, HSA14, HSA16 and HSA18; Fig. 4B; Table 3). The homologous pairs involving both peripheral and intermediate chromosomes distances were also further apart than the corresponding heterologous pairs (Fig. 4D; Table 3). For the two acrocentric chromosomes HSA14 and HSA21 that present intermediate and central localizations, respectively, the inter-homologue distances were also significantly larger than the inter-heterologue distances. The same was observed when we measured the distances between HSA21 and HSA16, a chromosome that presents a radial localization similar to HSA14 (Fig. 4E; Table 3). We do not observe any preferential proximity between the acrocentric chromosomes HSA14 and HSA21. This agrees with a previous study indicating that the mean distance between acrocentric chromosomes is similar to the distance between chromosomes with the same radial position (Bolzer et al., 2005). In theory, the largest inter-heterologue distances are likely to be observed between internal and peripheral chromosomes. We wondered whether, in this case, inter-homologue distances would still be larger than inter-heterologue distances. We thus examined the GC distances between internal (HSA17, HSA19) and peripheral (HSA1, HSA4) chromosomes (Fig. 4F). We indeed observed that the HSA1 and HSA4 inter-homologue distances were significantly larger than the inter-heterologue distances (HSA1–HSA17; HSA1–HSA19 and HSA4–HSA19) (Table 3). The same holds for the HSA17 inter-homologue distance, which

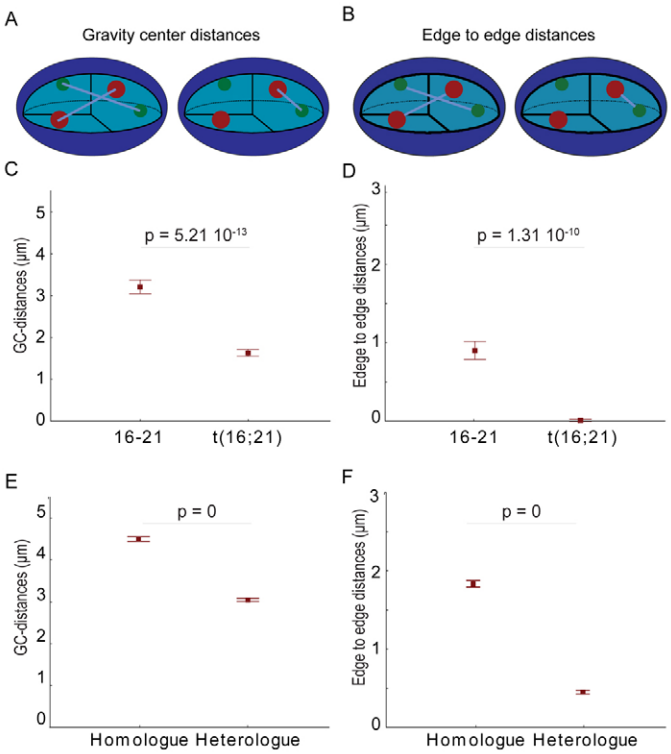

Fig. 3. Mean inter-heterologue distances are shorter than mean inter-homologue distances. The distances between the gravity centers (**A**) and between the edges (**B**) of either the four homologous CTs or of the two closest heterologous CTs have been measured. The mean distances between the gravity centers (GCs) (**C**) or between the edges (**D**) of the closest chromosome 16 and 21 were measured either in EJ-30 (16–21; n=70) or in ClH2 [t(16;21); n=60] cells. (**E**) The mean inter-heterologue and inter-homologue GC-distances were measured in the EJ-30 nucleus hybridized with the following pairs of probes (1–4; 1–16; 1–17; 4–16; 4–17; 4–19; 8–16; 10–16; 14–16; 14–21; 16–18; 16–21; 17–19 and 18–19, n=1200). (**F**) The mean inter-heterologue and inter-homologue distances between the edges of CTs were measured in the same hybridized EJ-30 nuclei (n=1200). The statistical significance was assessed using a Student's t-test (error bar=s.e.m.).

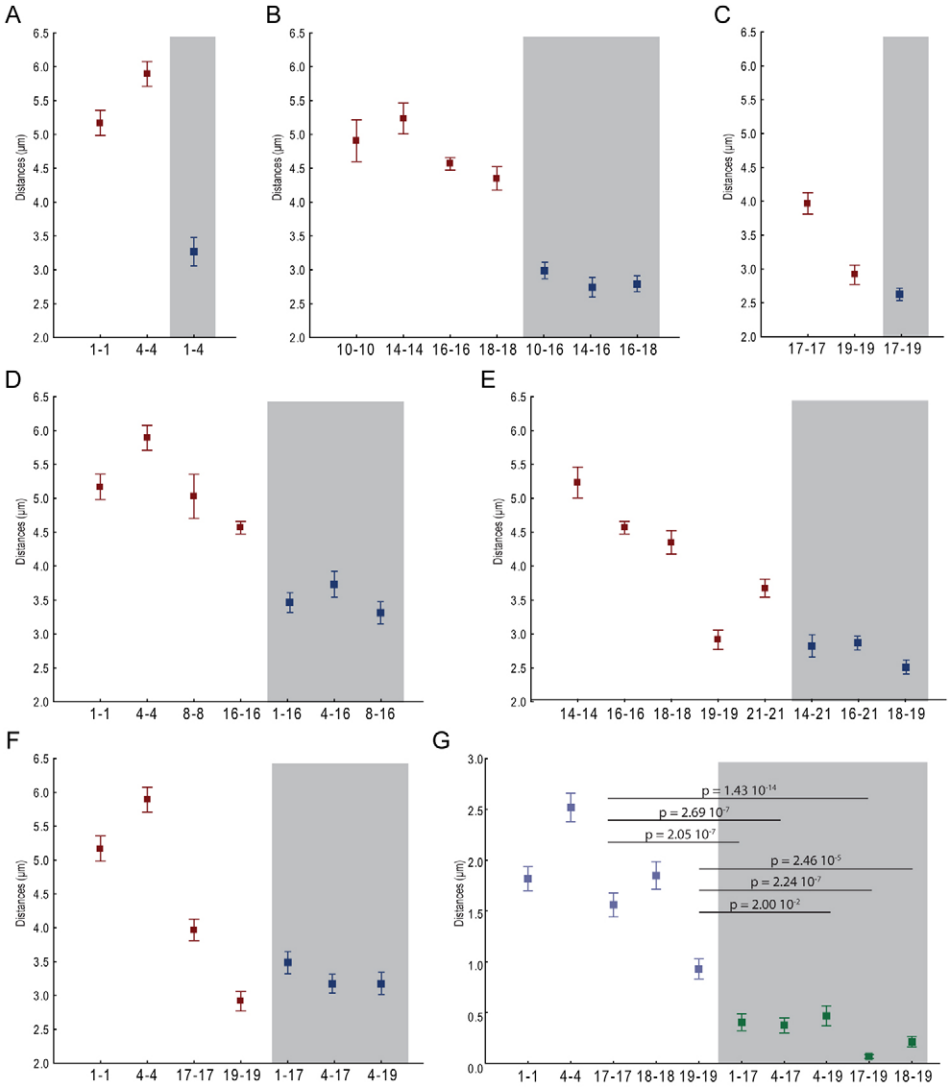

Fig. 4. A chromosome is generally closer to a heterologous chromosome than to its homologue. A pair wise comparison of inter-homologue and inter-heterologue GC-distances between CTs with specific radial position is presented (**A–F**). The GC-distances were measured (A) between two peripheral CTs (1–4, *n*=68), (B) between two intermediate CTs (10–16, *n*=82; 14–16, *n*=52; 16–18, *n*=97), (C) between two central chromosomes (17–19, *n*=100), (D) between peripheral and intermediate chromosomes (1–16, *n*=97; 4–16, *n*=68; 8–16, *n*=94), (E) between intermediate and central chromosomes (14–21, *n*=65; 16–21, *n*=163; 18–19, *n*=98) and (F) between central and peripheral chromosomes (1–17, *n*=76; 4–17, *n*=77; 4–19, *n*=73) (error bar=s.e.m.). (**G**) Pairwise comparison of inter-homologue and inter-heterologue edge-to-edge-distances between HSA1, HSA4, HSA17, HSA18 and HSA19 (1–17, *n*=76; 4–17, *n*=71; 4–19, *n*=73; 17–19, *n*=100; 18–19, *n*=98) (Student's *t*-test; error bar=s.e.m.).

was also significantly larger than the HSA4–HSA17 inter-heterologue distance. However, for some chromosomes pairs involving the most central chromosomes, the inter-heterologue distance was larger than the inter-homologue distance (HSA1–HSA17, HSA4–HSA19, HSA17–HSA19 and HSA18–HSA19) (Fig. 4C,E,F; Table 3). This could mean that centrally located chromosomes behave differently than others or rather reflect the underestimation of the inter-homologue GC-distances of these central chromosomes. Indeed for HSA17 and HSA19, respectively 18% and 30% of the nuclei exhibit a single FISH signal and were counted as having a GC-distance equal to zero (supplementary material Table S1).

As the measurements of distances between gravity centers clearly underestimate the proximity between homologous chromosomes, we determined the shortest distance between the borders of the chromosome territories by measuring the edge-to-edge distances. In this evaluation, there is no underestimation of inter-homologue distances. Measuring the distances between the borders of homologous and heterologous chromosomes in all nuclei, we observed that the mean distance between the closest heterologues (0.45±0.02 µm) is smaller than the distance between two homologous chromosomes (1.84±0.04 µm; *P*=0; Fig. 3F). When we compared two pairs of homologous chromosomes per nucleus, we confirmed the conclusion drawn from the comparison of GC-distances. In addition, we observed that the HSA17 inter-homologue edge-to-edge distance was significantly larger than both the HSA1–HSA17 and the HSA4–HSA17 inter-heterologue distance and the HSA19 inter-homologue distance was larger than the HSA4–HSA19, HSA17–HSA19 and HSA18–HSA19 inter-heterologue distances (Fig. 4G; supplementary material Fig. S1). Thus, the mean edge-to edge distance between the two closest heterologues is always smaller than the mean distance between homologues, even for the most centrally located chromosomes HSA17 and HSA19.

Both methods show that a chromosome is generally closer to a heterologue than to its homologue. The measure of edge-to-edge distances additionally shows that this is true even for internally located chromosomes.

Constrained or random organization of heterologues and homologues in the nucleus

The fact that the distances measured between homologues are larger than distances between heterologues could reflect an organizational constraint or be derived from a statistical bias.

Table 3. Statistical difference between inter-homologue and inter-heterologue GC distances

HSA pair	1–4	1–16	1–17	4–16	4–17	4–19	8–16
1–1	5.63×10^{-7}	6.10×10^{-8}	1.56×10^{-6}				
4–4	9.08×10^{-11}			4.69×10^{-8}	3.83×10^{-13}	1.91×10^{-12}	
8–8							4.70×10^{-6}
10–10							
14–14							
16–16		1.02×10^{-5}		4.79×10^{-3}			9.12×10^{-7}
17–17			**0.11**		7.50×10^{-3}		
18–18							
19–19						**0.37**	
21–21							

HSA pair	10–16	14–16	14–21	16–18	16–21	17–19	18–19
1–1							
4–4							
8–8							
10–10	4.98×10^{-8}						
14–14		7.67×10^{-11}	1.20×10^{-11}				
16–16	8.12×10^{-9}	8.51×10^{-8}		2.57×10^{-12}	2.22×10^{-17}		
17–17						3.07×10^{-7}	
18–18				8.41×10^{-9}			8.16×10^{-12}
19–19						**0.22**	**0.12**
21–21			1.74×10^{-3}		1.28×10^{-5}		

The statistical significance between inter-homologue and inter-heterologue GC-distances was assessed using a Student's *t*-test. Bold numbers correspond to nonsignificant differences ($P>0.05$).

Indeed, the fact that we compared the smallest of the four distances measured between heterologues with the unique distance measured between homologues could lead to this observation. To determine whether the observed distribution between homologous and heterologous chromosomes is expected given a random chromosomal organization, we compared the observed GC distances with distances measured on simulated patterns, where CTs were randomly and uniformly positioned in nuclei. Kolmogorov–Smirnov tests at level 5% showed that the observed distances were not all consistent with distances simulated based on a random and uniform position of CTs (data not shown). We then wondered whether CT preferential radial positioning alone could account for the observed distances. To answer this question, we designed simulations taking CT radial positioning into account. To this end, in each imaged nucleus, we simulated 999 patterns of four points in three dimensions. Each point was uniformly distributed on an orbit (surface at a constant distance to the nuclear envelope) defined by the position observed for each CT gravity center, and the four points were positioned independently (Fig. 5A). The comparison of the distribution of simulated distances with the distance observed defines the lower distance fraction (LDF) corresponding to the proportion of simulated distances smaller than the observed distance (Fig. 5B). In the case where an observed distance is consistent with simulated distances, the LDF is expected to be uniformly distributed between 0 (observed distance smaller than all simulated distances) and 1 (observed distance larger than all simulated distances). LDF histograms for two pairs of homologues and two pairs of heterologues are shown in Fig. 5C (complete histograms are shown in supplementary material Fig. S2). Kolmogorov–Smirnov tests at level 5% showed that the observed distances were consistent with simulated distances for HSA10, HSA16, HSA17, HSA18 and HSA19 (Fig. 5C; supplementary material Fig. S2), highlighting that the radial positioning of these chromosomes is sufficient to obtain the distribution of distances observed between homologues. However, for other chromosomes, the observed distances are not consistent with this model (Fig. 5C; supplementary material Fig. S2). Indeed, the observed distances tended to be larger than simulated distances for the most peripheral chromosomes, namely HSA1, HSA4 and HSA8, but smaller for HSA21. For HSA14, the LDF histogram reveals a bimodal distribution, suggesting that the observed distances are both larger and smaller than the simulated one. Globally, these results suggest that, in addition to the radial constraints, unknown factors are involved in maintaining the distance between some homologous chromosomes.

Distances between the closest heterologous pairs have been investigated based on a second series of simulations. The CT centers of chromosomes HSA1, HSA4, HSA8, HSA14 and HSA21 were not randomized on their orbits as this model of positioning was not consistent with the observed homologous distances. Therefore, for these simulations, the gravity centers of chromosomes HSA1, HSA4, HSA8, HSA14 and HSA21 were positioned at their observed locations in each nucleus, whereas the gravity centers of chromosomes HSA10, HSA16, HSA17, HSA18 and HSA19 were positioned randomly, uniformly and independently on their orbit. LDF histograms for pairs of closest heterologous chromosomes are shown in Fig. 5C and supplementary material Fig. S2. Kolmogorov–Smirnov tests at level 5% showed no consistency between the observed and simulated heterologous distances for the chromosome pairs HSA4–HSA17, HSA4–HSA19, HSA8–HSA16, HSA16–HSA21 and HSA18–HSA19. This reveals that a random arrangement within constrained orbits is not enough to explain the short distances observed for these chromosomes. In each of these cases, the simulated distances were larger than the ones observed, suggesting that an active mechanism independent of radial positioning constrains these pairs of heterologues to be close to each other. For the other pairs of heterologues (HSA1–HSA16, HSA1–HSA17, HSA4–HSA16, HSA10–HSA16, HSA14–HSA16, HSA16–HSA18 and HSA17–HSA19), the positioning of homologues is enough to justify the distribution of distances observed between heterologues.

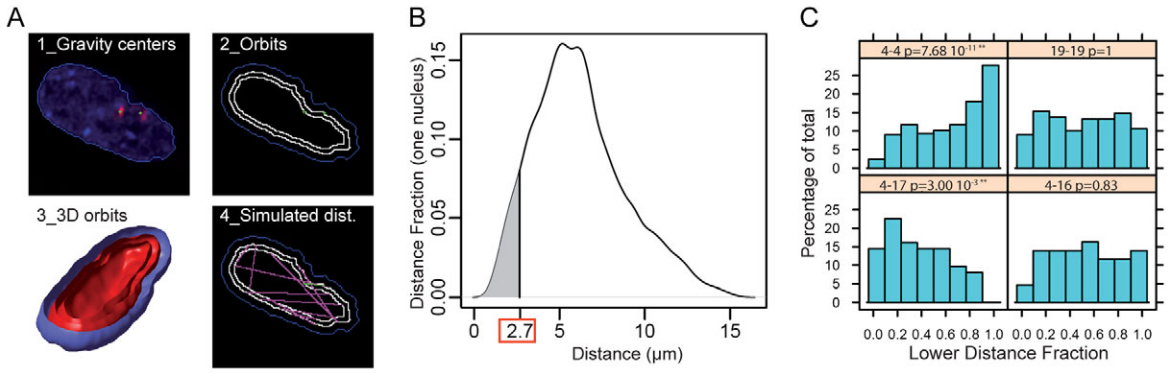

Fig. 5. Analysis of the random orbital positioning by three-dimensional numerical simulations. (**A**) Simulations of distances between chromosomes in each nucleus. (A1) For numerical simulations, each nucleus and CT were segmented and CT gravity centers were determined (green dot). (A2) The distances between gravity centers and the border of the nucleus were determined and used to define an orbit. (A3) An orbit corresponds to the surface at a constant distance from the nuclear envelope defined by the position observed for one of the CT gravity centers. (A4) A distribution of distances between chromosomes is simulated by a random, uniform and independent positioning of points on these orbits (red lines). (**B**) Each observed distance (outlined in red) was compared with the distribution of simulated distances (curve), and a lower-distance fraction (LDF, gray area) was defined for each nucleus. (**C**) Typical LDF histograms are shown (HSA4–HSA4; HSA19–HSA19; HSA4–HSA17; HSA4–HSA16). The *P*-value of the Kolmogorov–Smirnov test applied to determine whether the distance fraction deviates from a uniform distribution is given above each graph. Statistically significant differences are highlighted by asterisks.

The nucleolar organizer regions favor the internal positioning of chromosome 21

Our results show that the acrocentric chromosomes HSA14 and HSA21 particularly deviate from a random orbital arrangement (supplementary material Fig. S2). It is important to note that HSA14 and HSA21 are human acrocentric chromosomes and bear the nucleolar organizer regions (NORs) that have been proposed to be potential anchoring sites to the nucleolus (Hernandez-Verdun, 2006). Thus, the interaction with nucleoli that are centrally located in the nucleus, as shown by the assessment of the radial positioning of the B23 nucleolar specific protein (Fig. 6A,B), could constrain the position of HSA21. To evaluate the contribution of this interaction to chromosome positioning, we used a subclone of the EJ-30 cell line (ClH2 cells) that contains a single additional translocation involving HSA16 and HSA21 – t(16;21). The hybridization of metaphase spreads of the ClH2 subclone with probes specific for nucleolar organizer regions (NORs) revealed that the acrocentric chromosome 21 involved in the translocation t(16;21) is missing its NORs (Fig. 6C,D). Additional cytogenetic experiments indicated that, besides the deletion of the short arm of chromosome 21 bearing NORs, the translocated fragment corresponds to most of the long arm of the chromosome 21 with no detectable rearrangements. Indeed, the HSA21 centromere was absent but the 21q22 and the subtelomeric regions were present at the end of the translocated chromosome (supplementary material Fig. S3). The evaluation of the radial position of the HSA21-specific signal corresponding to both the normal HSA21 chromosome and the HSA21 fragment involved in the translocation with HSA16 (hereafter named t21) showed that the distribution of HSA21 shifted towards a more peripheral position in ClH2 cells compared with EJ-30 cells (P=1.48×10^{-4}; Fig. 6E). Concomitantly, the radial positioning of the HSA16 signals was not significantly modified (P=0.34; Fig. 6E). To determine whether the position of both HSA21 and t21 was modified, we analyzed the radial position of each chromosome independently. These are distinguishable in ClH2 cells based on their distance with the chromosome 16 staining (Fig. 6F). Fig. 6G shows that, whereas the position HSA21 is not modified, t21 localizes more peripherally in ClH2 cells (P=2.00×10^{-3}; Fig. 6G). It is noteworthy that t21 becomes more peripheral than t16 (P=1.26×10^{-2}; Fig. 6G), showing that t21 is not simply dragged to the periphery by its translocation partner. This change in radial position is particularly striking as, using the same approach, we observe no change in the radial position of the chromosomes 8 and 10 that bear small translocations (supplementary material Fig. S4). Altogether, these observations suggest that the normal HSA21 chromosomes are actively constrained at the center of the nucleus and that the absence of anchoring sequences on t21 allows this chromosome to relocate more peripherally. Even if we cannot completely exclude that other sequences absent from the translocated fragment of the chromosome 21 are involved in the central anchoring of HSA21, NORs are good candidates to mediate a central anchoring by means of their interaction with nucleoli. In this case, one prediction is that, in EJ-30 cells, both HSA21 homologues might interact with nucleoli, whereas t21 should not in ClH2 cells. We indeed observed that both HSA21 chromosomes are nearby nucleoli in 100% of EJ-30 cells, whereas a chromosome 21 is far away from the nucleoli in 89% of ClH2 cells, showing that the loss of NOR sequences correlates with a loss of interaction with nucleoli (supplementary material Fig. S5). In the absence of internal anchoring sites, the peripheral relocalization of t21 could simply reflect the positioning of t21 relative to its gene density or size. However, the median radial position adopted by the t21 chromosome (72.5) is larger than the radial position expected for HSA21 based on the linear regressions determined in Fig. 2 (59.8, 70.5 or 63.6 for a correlation with the size, gene density or gene density/size, respectively). Overall, these results suggest that, in addition to NOR internal anchoring sequences, HSA21 bears secondary peripheral anchoring sites that are revealed in the absence of the primary one.

Discussion

A gene-density-correlated nuclear architecture was initially described for entire CTs in spherically shaped nuclei of lymphocytes (Boyle et al., 2001; Cremer et al., 2001; Croft et al., 1999). For flat ellipsoid nuclei of fibroblasts, several studies described a chromosome-size-correlated radial CT arrangement in quiescent

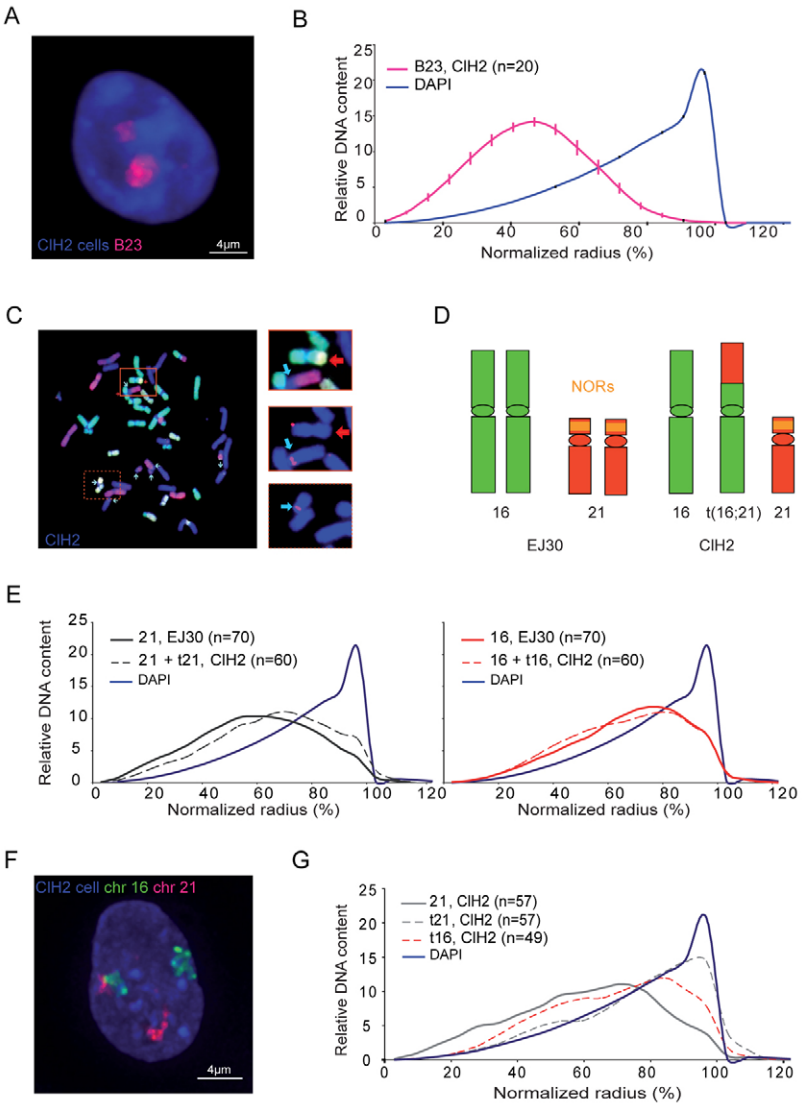

Fig. 6. Involvement of nucleolar organizer regions (NORs) in the radial positioning of HSA21. (**A**) Nucleoli were labeled by immunostaining of the nucleophosmin (B23 protein) in ClH2 cells, and (**B**) their relative radial positioning was determined (error bar=s.e.m.). (**C**) HSA21-specific signals were identified by M-FISH analysis (yellow signal), and NORs were labeled using specific probes on metaphase spreads of ClH2 cells. HSA21 and t(16;21) are framed by dashed and unbroken red squares, respectively. The two first insets correspond to the magnification of t(16;21) visualized with M-FISH (top inset) and after hybridization with NOR-specific probes (middle inset). The lower inset shows a magnification of the untranslocated HSA21 hybridized with NOR-specific probes. (**D**) Scheme of chromosomes 16 (green) and 21 (red) in the EJ-30 and ClH2 cells. NORs on the short arm of HSA21 are represented by an orange box. (**E**) The RRD of the chromosomes 21 (gray) and 16 (red) were determined in EJ-30 nuclei (unbroken lines, *n*=70) and in ClH2 nuclei (broken lines, *n*=60). (**F**) ClH2 nuclei were hybridized with probes against HSA16 (green) and HSA21 (magenta). (**G**) The RRD of the untranslocated HSA21 (21, solid gray line, *n*=57), of the translocated chromosome 21 (t21, broken gray line, *n*=57) and of the translocated chromosome 16 (t16, broken red line, *n*=49) were assessed in ClH2 cells.

cells (Bolzer et al., 2005; Cremer et al., 2001; Croft et al., 1999), whereas a more gene-density-correlated arrangement was reported in cycling cells (Bridger et al., 2000). Based on the analysis of only two chromosomes, HSA18 and HSA19, it was previously proposed that chromosomes are arranged relative to their chromosome size in epithelial cells from amniotic fluid (Bolzer et al., 2005). In the present study, based on the analysis of more than 1600 nuclei for 10 chromosomes, we demonstrated that the radial arrangement of chromosome territories correlates equally well with gene density and chromosome size for human epithelial cells isolated from a bladder carcinoma. Despite the fact that chromosome spatial organization has been shown to vary between different cell types (Parada et al., 2004), a gene density- and chromosome size-correlated arrangement is not specific to epithelial cells, as these two parameters have been shown to influence chromosome intranuclear position in human and monkey fibroblasts (Mora et al., 2006).

How gene density and/or chromosome size influence chromosome localization is currently unknown. Whether the influence of the gene density on chromosome positioning actually reflects transcriptional activity is still a matter of debate. However, it seems clear that the nuclear interior has a particular competence for gene expression. An internal positioning of actively transcribed genes has been described (Lukasova et al., 2002; Scheuermann et al., 2004; Zink et al., 2004). This tendency seems to extend to whole chromosomes as transcriptome studies reveal that chromosomal territories rich in highly expressed genes are located in the nuclear interior (Kozubek et al., 2002). However, highly expressed genes located in a gene-poor environment can well be found at the nuclear periphery (Brown et al., 2006; Kupper et al., 2007). The contribution of chromosome size to radial positioning is more difficult to interpret. Three-dimensional modeling of CT arrangements based on a linear relationship between chromosome size and CT volume has shown that topological constraints do not play a decisive role in radial positioning (Cremer et al., 2001). Our new observation that radial positioning correlates better with a new parameter corresponding to the ratio of gene density to chromosome size shows that both parameters influence radial positioning. The fact that radial position is inversely correlated with the square of the chromosome size could somehow reflect a contribution of the spatial conformation of CTs. We also observed that chromosome size correlates with the frequency of repeated elements (data not

shown). Interestingly, among these repeated elements, Alu sequences that are interspersed in gene-dense regions have been shown to localize preferentially in the nuclear interior (Bolzer et al., 2005). Other repeated sequences, such as telomeres that have been shown to interact with the nuclear matrix (de Lange, 1992; Luderus et al., 1996; Pierron and Puvion-Dutilleul, 1999; Weipoltshammer et al., 1999), could as well present particular positions in the nucleus and influence the position of whole chromosomes.

Among the repeated sequences, rDNA has long been proposed to serve as an anchor through its interaction with nucleoli. In human cells, this assertion was based on the observation that acrocentric chromosomes were often centrally located and exhibited short inter-homologue distances (Bolzer et al., 2005; Chandley et al., 1996). In support of this hypothesis, our results show that a fragment of HSA21 missing the NOR sequences relocates towards a more peripheral position. In addition, the HSA21 fragment translocated onto HSA16 does not simply adopt the position of its translocation partner but becomes even more peripheral. What targets HSA21 to the nuclear periphery is unclear. Nucleoli, when internally located in the nucleus, have been shown to be in contact with nuclear membrane convolutions (Bourgeois and Hubert, 1988). Thus, one possibility is that HSA21 contains both nucleolar and nuclear membrane anchoring sites. Whether this is also true for other acrocentric chromosomes remains to be determined. However, the fact that HSA14 inter-homologue distances can be both smaller and larger than the simulated distances suggests that it might be the case.

In addition to the radial arrangement of chromosome territories, we observed a particular arrangement of homologous versus heterologous chromosomes. We found out that a chromosome is generally closer to a heterologous chromosome than to its homologue. Indeed, measured inter-homologue distances are, for the pairs we studied, significantly larger than inter-heterologue distances. This has also been observed in the mouse (Caddle et al., 2007), and mathematical simulations have shown that this assembly in heterologous neighborhoods reflects a non-random positioning of chromosome territories (Khalil et al., 2007). However, it was not addressed whether this was a direct consequence of the radial arrangement of chromosomes in the nucleus. By using numerical simulation models taking into account the radial position of chromosomes, we showed that a radial organization can effectively, in some cases, justify the distribution of the observed inter-homologue distances. However, our model of positioning was not consistent with the observed homologous distances for the most peripheral chromosomes (HSA1, HSA4 and HSA8). Rejection of the model might be caused by non-independent positioning of homologous CTs, by a spatial heterogeneity of anchoring sites at the nuclear periphery or by both causes. Interestingly, HSA4 bears the D4Z4 sequences that have been proposed to be peripheral anchors (Masny et al., 2004; Ottaviani et al., 2009). The model of positioning was also rejected for the acrocentric chromosome HSA21 because the distances between homologues were smaller than those predicted by the simulations. This could reflect the anchoring of both HSA21 homologues to the same nucleolar compartment. The picture is more complex for the HSA14 acrocentric chromosome for which distances both smaller and larger than predicted by the simulations are observed. This bimodal distribution could reflect different behaviors of HSA14 homologues relative to their association with differently positioned nucleoli.

The fact that the preferential association of heterologous chromosomes and the separation of homologues is a conserved feature in murine and human cells suggests that this relative positioning could be of functional importance. A large distance between homologues could avoid homologous recombination and subsequent potentially deleterious loss of heterozygosity. This is consistent with the fact that homologous rearrangements have been shown to be infrequent after irradiation in both murine and human cells (Boei et al., 2006; Caddle et al., 2007), although the accurate detection of rearrangements between homologues is questionable. However, considering the number of repeated sequences in mammalian genomes, proximity of heterologous chromosomes could also produce deleterious homologous recombination events. In addition, heterologous neighborhoods could favor repair events leading to large-scale genome rearrangements. An alternative is that maintaining homologues at a distance would avoid damaging both copies of a gene by environmental or intrinsic stresses such as irradiation, reactive oxygen species, replication or transcription.

An increasing body of evidence, coming from both FISH and recent 3C or 4C experiments, supports the fact that physical interaction between loci influences the regulation of gene expression. The most striking example is the somatic pairing of homologous chromosomes observed in Diptera that strongly impacts, positively or negatively, the regulation of gene transcription through a mechanism called transvection (Duncan, 2002). In mammals, such a general somatic pairing has not been observed. However, spatial clustering of active loci at transcription factories or at splicing-factor-rich speckles has been described (Brown et al., 2008; Brown et al., 2006; Hu et al., 2009; Osborne et al., 2004; Shopland et al., 2006) and could relate to the preferential proximity we observe between heterologous chromosomes. By contrast, maintaining homologous chromosomes at a distance could avoid co-regulation of both alleles. Supporting this hypothesis, an abnormal pairing of homologous HSA19 chromosomes has been reported in renal oncocytoma cells and was shown to correlate with a significant increase in the transcription of the paired region, suggesting that separation of homologous loci can take part in the regulation of gene expression (Koeman et al., 2008). More generally, the fact that the numerous human genes (300 out of 4000 tested) that exhibit monoallelic expression are scattered throughout the entire genome (Gimelbrant et al., 2007) supports the hypothesis that a general dispersion of homologous chromosomes is required to avoid transcriptional coregulation of these alleles.

Interestingly, transient homologous pairings have been observed in particular developmental contexts and were associated with allelic differential regulation. During early embryogenesis of female mammals, a transient somatic pairing has been shown to occur between homologous X chromosomes as part of the X inactivation process (Augui et al., 2007; Bacher et al., 2006; Xu et al., 2006). A temporary pairing of homologous immunoglobulin genes also occurs during the development of B cells and is associated with the subsequent monoallelic recombination and transcription of these loci (Hewitt et al., 2009). In the light of these findings, one appealing model is that separation of homologous chromosomes would allow for maintenance of two copies of monoallelically expressed genes at a distance, avoiding their co-regulation, whereas active mechanisms would dynamically control transient interchromosomal contacts required to set up this differential allelic expression.

Materials and Methods

Cell lines and cell culture

The EJ-30 cell line, also named MGH-U1 (O'Toole et al., 1983), was subcloned from the EJ epithelial bladder cell carcinoma cell line. This cell line is telomerase positive and p53 negative. EJ-30 cells contain the following chromosome aberrations: del4q, t(7;8), del9p, t(10;22), t(11;20), t(15;18), del22q. ClH2 cells were subcloned from EJ-30 cells and present the same karyotype as EJ-30 cells with an additional translocation t(16;21). Cells were grown in alpha minimal essential medium with glutamax (Gibco) supplemented with 10% fetal calf serum (Gibco) and 1× antibiotic–antimycotic solution (Gibco). The karyotype was checked at each 3D FISH experiment by M-FISH. We frequently observed polyploid cells that were eliminated from our analyses based on the presence of more than two painted homologous chromosomes. For microscopy, cells were cultivated for 18 hours on coverslips (0.17±0.01 mm, Hecht-Assistent).

Fluorescence in situ hybridization and probes

Fluorescence in situ hybridizations were performed as described previously (Cremer et al., 2001). Commercial Texas Red- and FITC-labeled whole-chromosome painting probes for human chromosomes 1, 4, 8, 10, 14, 16, 17, 18, 19 and 21 were supplied ready-to-use in a hybridization mixture (MetaSystems) and used as described in the technical description of the supplier. The nuclei were counterstained in 0.5 $\mu g.ml^{-1}$ 4,6 diamidino-2-phenylindole (DAPI) and slides were mounted in *p*-phenylenediamine (PPD).

Immunofluorescence experiments with the primary antibody anti-B23 (H-106; Santa Cruz Biotechnology) were performed as described previously (Campalans et al., 2005). Immuno-FISH experiments with the labeling of nucleoli (anti-C23, MS-3; Santa Cruz Biotechnology) were performed as described previously (Zinner et al., 2007).

The preparation of chromosomes and cytogenetic analysis by FISH were performed as described previously (Sabatier et al., 2005). The probes specific for HSA21 centromere (Amplitech), region 21q22 (Kreatech) and subtelomeres of HSA21 long arm (Aquarius) were labeled according to the manufacturers' instructions. The labeling of the nucleolar organizer region was performed with the pA probe. The pA probe contains the 3′ end of 18S rDNA, the 5.8S rDNA, both internal transcribed spacers and most of the 28S rDNA. The probes were labeled by biotin using a nick-translation kit (Roche) according to the manufacturer's instructions.

Microscopy

An Olympus IX81 microscope (×100 objectives, Zeiss) with a Cool-SNAP-HQ camera (Princetown Instrument) and an electric piezo (PIFOC, PI) driven by Metamorph software 6.2.1 (Universal Imaging Corp.) was used to capture 80-image stacks of 250 nm step size. A deconvolution was performed using Metamorph Software with the following parameters: fast algorithm with five iterations, sigma 0.7 and a frequency of 4 using HTP-deconvolution program. For capture of confocal images, a Zeiss LSM 510 microscope with ×63 PlanApochromat 1.4 NA oil immersion objectives (Zeiss) was used to acquire 40- to 50-image stacks of 203 nm step size.

Image processing and analysis

A low-pass filtering (5×3) and a median filtering [3×3, sub-sample ratio 1 (radius 1.6)] were applied for nucleus and CT stacks, respectively. Image stacks were normalized and transformed in 8 bit. A first threshold was manually determined using ImageJ software. For nuclei in which homologous chromosomes were not separated by this threshold, a watershed-based split provided by the ITK library, taking into account the intensity and shape of the signal, was applied. For each chromosome, 200 nuclei were analyzed on average, distributed into three experiments. To check that there were no statistical differences between experiments for a given chromosome, we compared the percentage of associated homologues, the volume of chromosome territories, and the volume of nuclei.

Relative radial distribution: the relative radial distributions (RRDs) of chromosome territories were determined as described previously (Cremer et al., 2001). Pair-wise comparisons were performed using nonparametric multivariate tests based on marginal ranks, as described previously (Puri and Sen, 1971), and implemented in the R package ICSNP. For the comparison of chromosomes imaged together in the same nuclei, RRD differences were computed shell-by-shell for each nucleus, and a null mean difference was tested. For the comparison of chromosomes not imaged together, a two-sample location test was performed. There are some pairs of chromosomes where both tests could be performed, yielding two P values P_1 and P_2. The global P value was computed as $P_1P_2–P_1P_2\log(P_1P_2)$.

Evaluation of distances between gravity centers of chromosome territories: the gravity centers of signals were determined with the 3D Objects counter plug-in (F. P. Cordelières) for ImageJ software (Rasband, W.S., ImageJ, NIH, Bethesda, MD, http://rsb.info.nih.gov/ij/, 1997–2007) that has already been used by others (Teller et al., 2007). For the chromosomes segmented by the watershed-based approach, the gravity centers were determined using ITK.

Evaluation of edge-to-edge distances: edge-to-edge distances were assessed using the absolute distance to surface (ADS) program (Khalil et al., 2007; Solovei et al., 2009). This program allowed for quantification of the shortest distance of given sub-CT units with respect to a boundary structure in 3D. In each nucleus, the outlines of chromosome territories were determined, and concentric shells with equivalent radii were defined for each object. For each CT, the shell containing the first pixel of another CT was determined, and the corresponding distance was calculated. In these evaluations, overlapping heterologues or homologues result in a null distance. The statistical significance of the inter-homologue and inter-heterologue distances was tested using Student's *t*-test.

Numerical simulations

Orbits of CT gravity centers have been computed from nuclear distance maps. Random sampling of orbits was based on surface-area maps associated with the orbits (Legland et al., 2007). Simulated CT centers were drawn randomly and independently of each other on orbits. Only CT distances above a minimal value that was chosen as the sum of two CT 'hardcore' radii were accepted for the further calculations. CT hardcore radii were determined from the smallest observed distances between CTs. As the smallest distances between homologous CTs were expected to be overestimated owing to the nonseparation of very close homologous CTs, they were given less weight than the smallest heterologous distances. The images with inseparable homologues were not included in the simulations of inter-homologue or inter-heterologue distances. The distance observed in each nucleus was compared with the distribution of simulated distances. A Kolmogorov–Smirnov test, followed by a *P*-value correction controlling of the false discovery rate (Benjamini and Yekutieli, 2001), was applied to determine whether the distribution of lower distance fractions deviates from a uniform distribution. Simulations have been performed using the Insight Segmentation and Registration Toolkit Library (ITK) and its Python interface WrapITK.

The EJ-30 cell line was kindly provided by John Murnane and William Dewey (University of California, San Francisco, CA). We are grateful to Fabrice Cordelières (Cell and Tissue Imaging Facility, Curie Institute, Orsay, France) for his help in image analysis, to Gaëtan Lehmann (Developmental Biology and Reproduction, INRA, Jouy-en-Josas, France) for his support on the programming ITK library used for the simulations, to Angela Taddei (Nuclear Dynamics and Genome Plasticity UMR218, Institut Curie, Paris, France) and Gregor Kreth (KIP, Heidelberg University, Germany) for helpful discussions and to Grace Shim (Radiobiology and Oncology, CEA), Elphège Nora and Jennifer Chow (Developmental Biology and Genetics, Curie Institute, Paris, France) for critically reading the manuscript. Claire Heride was supported by a PhD fellowship from ED418 and ARC. This work was supported by RISC-RAD contract number FI6R-CT2003-508842.

Supplementary material available online at
http://jcs.biologists.org/cgi/content/full/123/23/4063/DC1

References

Augui, S., Filion, G. J., Huart, S., Nora, E., Guggiari, M., Maresca, M., Stewart, A. F. and Heard, E. (2007). Sensing X chromosome pairs before X inactivation via a novel X-pairing region of the Xic. *Science* **318**, 1632-1636.

Bacher, C. P., Guggiari, M., Brors, B., Augui, S., Clerc, P., Avner, P., Eils, R. and Heard, E. (2006). Transient colocalization of X-inactivation centres accompanies the initiation of X inactivation. *Nat. Cell Biol.* **8**, 293-299.

Benjamini, Y. and Yekutieli, D. (2001). The control of the false discovery rate in multiple testing under dependency. *Ann. Stat.* **29**, 24.

Boei, J. J., Fomina, J., Darroudi, F., Nagelkerke, N. J. and Mullenders, L. H. (2006). Interphase chromosome positioning affects the spectrum of radiation-induced chromosomal aberrations. *Radiat. Res.* **166**, 319-326.

Bolzer, A., Kreth, G., Solovei, I., Koehler, D., Saracoglu, K., Fauth, C., Muller, S., Eils, R., Cremer, C., Speicher, M. R. et al. (2005). Three-dimensional maps of all chromosomes in human male fibroblast nuclei and prometaphase rosettes. *PLoS Biol.* **3**, e157.

Bourgeois, C. A. and Hubert, J. (1988). Spatial relationship between the nucleolus and the nuclear envelope: structural aspects and functional significance. *Int. Rev. Cytol.* **111**, 1-52.

Boyle, S., Gilchrist, S., Bridger, J. M., Mahy, N. L., Ellis, J. A. and Bickmore, W. A. (2001). The spatial organization of human chromosomes within the nuclei of normal and emerin-mutant cells. *Hum. Mol. Genet.* **10**, 211-219.

Bridger, J. M., Boyle, S., Kill, I. R. and Bickmore, W. A. (2000). Re-modelling of nuclear architecture in quiescent and senescent human fibroblasts. *Curr. Biol.* **10**, 149-152.

Brown, J. M., Leach, J., Reittie, J. E., Atzberger, A., Lee-Prudhoe, J., Wood, W. G., Higgs, D. R., Iborra, F. J. and Buckle, V. J. (2006). Coregulated human globin genes are frequently in spatial proximity when active. *J. Cell Biol.* **172**, 177-187.

Brown, J. M., Green, J., das Neves, R. P., Wallace, H. A., Smith, A. J., Hughes, J., Gray, N., Taylor, S., Wood, W. G., Higgs, D. R. et al. (2008). Association between active genes occurs at nuclear speckles and is modulated by chromatin environment. *J. Cell Biol.* **182**, 1083-1097.

Bystricky, K., Heun, P., Gehlen, L., Langowski, J. and Gasser, S. M. (2004). Long-range compaction and flexibility of interphase chromatin in budding yeast analyzed by high-resolution imaging techniques. *Proc. Natl. Acad. Sci. USA* **101**, 16495-16500.

Bystricky, K., Laroche, T., van Houwe, G., Blaszczyk, M. and Gasser, S. M. (2005). Chromosome looping in yeast: telomere pairing and coordinated movement reflect anchoring efficiency and territorial organization. *J. Cell Biol.* **168**, 375-387.

Caddle, L. B., Grant, J. L., Szatkiewicz, J., van Hase, J., Shirley, B. J., Bewersdorf, J., Cremer, C., Arneodo, A., Khalil, A. and Mills, K. D. (2007). Chromosome neighborhood composition determines translocation outcomes after exposure to high-dose radiation in primary cells. *Chromosome Res.* **15**, 1061-1073.

Campalans, A., Marsin, S., Nakabeppu, Y., O'Connor, T. R., Boiteux, S. and Radicella, J. P. (2005). XRCC1 interactions with multiple DNA glycosylases: a model for its recruitment to base excision repair. *DNA Rep.* **4**, 826-835.

Chandley, A. C., Speed, R. M. and Leitch, A. R. (1996). Different distributions of homologous chromosomes in adult human Sertoli cells and in lymphocytes signify nuclear differentiation. *J. Cell Sci.* **109**, 773-776.

Cornforth, M. N., Greulich-Bode, K. M., Loucas, B. D., Arsuaga, J., Vazquez, M., Sachs, R. K., Bruckner, M., Molls, M., Hahnfeldt, P., Hlatky, L. et al. (2002). Chromosomes are predominantly located randomly with respect to each other in interphase human cells. *J. Cell Biol.* **159**, 237-244.

Cremer, T. and Cremer, C. (2001). Chromosome territories, nuclear architecture and gene regulation in mammalian cells. *Nat. Rev. Genet.* **2**, 292-301.

Cremer, T., Cremer, C., Schneider, T., Baumann, H., Hens, L. and Kirsch-Volders, M. (1982). Analysis of chromosome positions in the interphase nucleus of Chinese hamster cells by laser-UV-microirradiation experiments. *Hum. Genet.* **62**, 201-209.

Cremer, T., Kurz, A., Zirbel, R., Dietzel, S., Rinke, B., Schrock, E., Speicher, M. R., Mathieu, U., Jauch, A., Emmerich, P. et al. (1993). Role of chromosome territories in the functional compartmentalization of the cell nucleus. *Cold Spring Harbor Symp. Quant. Biol.* **58**, 777-792.

Cremer, M., von Hase, J., Volm, T., Brero, A., Kreth, G., Walter, J., Fischer, C., Solovei, I., Cremer, C. and Cremer, T. (2001). Non-random radial higher-order chromatin arrangements in nuclei of diploid human cells. *Chromosome Res.* **9**, 541-567.

Cremer, M., Kupper, K., Wagler, B., Wizelman, L., von Hase, J., Weiland, Y., Kreja, L., Diebold, J., Speicher, M. R. and Cremer, T. (2003). Inheritance of gene density-related higher order chromatin arrangements in normal and tumor cell nuclei. *J. Cell Biol.* **162**, 809-820.

Croft, J. A., Bridger, J. M., Boyle, S., Perry, P., Teague, P. and Bickmore, W. A. (1999). Differences in the localization and morphology of chromosomes in the human nucleus. *J. Cell Biol.* **145**, 1119-1131.

de Lange, T. (1992). Human telomeres are attached to the nuclear matrix. *EMBO J.* **11**, 717-724.

Duncan, I. W. (2002). Transvection effects in Drosophila. *Annu. Rev. Genet.* **36**, 521-556.

Finlan, L. E., Sproul, D., Thomson, I., Boyle, S., Kerr, E., Perry, P., Ylstra, B., Chubb, J. R. and Bickmore, W. A. (2008). Recruitment to the nuclear periphery can alter expression of genes in human cells. *PLoS Genet.* **4**, e1000039.

Gilbert, N., Gilchrist, S. and Bickmore, W. A. (2005). Chromatin organization in the mammalian nucleus. *Int. Rev. Cytol.* **242**, 283-336.

Gimelbrant, A., Hutchinson, J. N., Thompson, B. R. and Chess, A. (2007). Widespread monoallelic expression on human autosomes. *Science* **318**, 1136-1140.

Gotta, M. and Gasser, S. M. (1996). Nuclear organization and transcriptional silencing in yeast. *Experientia* **52**, 1136-1147.

Guacci, V., Hogan, E. and Koshland, D. (1997). Centromere position in budding yeast: evidence for anaphase A. *Mol. Biol. Cell* **8**, 957-972.

Guelen, L., Pagie, L., Brasset, E., Meuleman, W., Faza, M. B., Talhout, W., Eussen, B. H., de Klein, A., Wessels, L., de Laat, W. et al. (2008). Domain organization of human chromosomes revealed by mapping of nuclear lamina interactions. *Nature* **453**, 948-951.

Habermann, F. A., Cremer, M., Walter, J., Kreth, G., von Hase, J., Bauer, K., Wienberg, J., Cremer, C., Cremer, T. and Solovei, I. (2001). Arrangements of macro- and microchromosomes in chicken cells. *Chromosome Res.* **9**, 569-584.

Hernandez-Verdun, D. (2006). The nucleolus: a model for the organization of nuclear functions. *Histochem. Cell Biol.* **126**, 135-148.

Heun, P., Taddei, A. and Gasser, S. M. (2001). From snapshots to moving pictures: new perspectives on nuclear organization. *Trends Cell Biol.* **11**, 519-525.

Hewitt, S. L., Yin, B., Ji, Y., Chaumeil, J., Marszalek, K., Tenthorey, J., Salvagiotto, G., Steinel, N., Ramsey, L. B., Ghysdael, J. et al. (2009). RAG-1 and ATM coordinate monoallelic recombination and nuclear positioning of immunoglobulin loci. *Nat. Immunol.* **10**, 655-664.

Hu, Y., Kireev, I., Plutz, M., Ashourian, N. and Belmont, A. S. (2009). Large-scale chromatin structure of inducible genes: transcription on a condensed, linear template. *J. Cell Biol.* **185**, 87-100.

Jin, Q., Trelles-Sticken, E., Scherthan, H. and Loidl, J. (1998). Yeast nuclei display prominent centromere clustering that is reduced in nondividing cells and in meiotic prophase. *J. Cell Biol.* **141**, 21-29.

Khalil, A., Grant, J. L., Caddle, L. B., Atzema, E., Mills, K. D. and Arneodo, A. (2007). Chromosome territories have a highly nonspherical morphology and nonrandom positioning. *Chromosome Res.* **15**, 899-916.

Koeman, J. M., Russell, R. C., Tan, M. H., Petillo, D., Westphal, M., Koelzer, K., Metcalf, J. L., Zhang, Z., Matsuda, D., Dykema, K. J. et al. (2008). Somatic pairing of chromosome 19 in renal oncocytoma is associated with deregulated EGLN2-mediated [corrected] oxygen-sensing response. *PLoS Genet.* **4**, e1000176.

Kozubek, S., Lukasova, E., Jirsova, P., Koutna, I., Kozubek, M., Ganova, A., Bartova, E., Falk, M. and Pasekova, R. (2002). 3D Structure of the human genome: order in randomness. *Chromosoma* **111**, 321-331.

Kupper, K., Kolbl, A., Biener, D., Dittrich, S., von Hase, J., Thormeyer, T., Fiegler, H., Carter, N. P., Speicher, M. R., Cremer, T. et al. (2007). Radial chromatin positioning is shaped by local gene density, not by gene expression. *Chromosoma* **116**, 285-306.

Legland, D., Kieu, K. and Devaux, M. (2007). Computation of Minkowski measures on 2D and 3D binary images. *Image Anal. Stereology* **26**, 83-92.

Lieberman-Aiden, E., van Berkum, N. L., Williams, L., Imakaev, M., Ragoczy, T., Telling, A., Amit, I., Lajoie, B. R., Sabo, P. J., Dorschner, M. O. et al. (2009). Comprehensive mapping of long-range interactions reveals folding principles of the human genome. *Science* **326**, 289-293.

Luderus, M. E., van Steensel, B., Chong, L., Sibon, O. C., Cremers, F. F. and de Lange, T. (1996). Structure, subnuclear distribution, and nuclear matrix association of the mammalian telomeric complex. *J. Cell Biol.* **135**, 867-881.

Lukasova, E., Kozubek, S., Kozubek, M., Falk, M. and Amrichova, J. (2002). The 3D structure of human chromosomes in cell nuclei. *Chromosome Res.* **10**, 535-548.

Malhas, A., Lee, C. F., Sanders, R., Saunders, N. J. and Vaux, D. J. (2007). Defects in lamin B1 expression or processing affect interphase chromosome position and gene expression. *J. Cell Biol.* **176**, 593-603.

Masny, P. S., Bengtsson, U., Chung, S. A., Martin, J. H., van Engelen, B., van der Maarel, S. M. and Winokur, S. T. (2004). Localization of 4q35.2 to the nuclear periphery: is FSHD a nuclear envelope disease? *Hum. Mol. Genet.* **13**, 1857-1871.

Mayer, R., Brero, A., von Hase, J., Schroeder, T., Cremer, T. and Dietzel, S. (2005). Common themes and cell type specific variations of higher order chromatin arrangements in the mouse. *BMC Cell Biol.* **6**, 44.

Meaburn, K. J., Cabuy, E., Bonne, G., Levy, N., Morris, G. E., Novelli, G., Kill, I. R. and Bridger, J. M. (2007). Primary laminopathy fibroblasts display altered genome organization and apoptosis. *Aging Cell* **6**, 139-153.

Mora, L., Sanchez, I., Garcia, M. and Ponsa, M. (2006). Chromosome territory positioning of conserved homologous chromosomes in different primate species. *Chromosoma* **115**, 367-375.

Nagele, R. G., Freeman, T., McMorrow, L., Thomson, Z., Kitson-Wind, K. and Lee, H. (1999). Chromosomes exhibit preferential positioning in nuclei of quiescent human cells. *J. Cell Sci.* **112**, 525-535.

Neusser, M., Schubel, V., Koch, A., Cremer, T. and Muller, S. (2007). Evolutionarily conserved, cell type and species-specific higher order chromatin arrangements in interphase nuclei of primates. *Chromosoma* **116**, 307-320.

O'Toole, C. M., Povey, S., Hepburn, P. and Franks, L. M. (1983). Identity of some human bladder cancer cell lines. *Nature* **301**, 429-430.

Osborne, C. S., Chakalova, L., Brown, K. E., Carter, D., Horton, A., Debrand, E., Goyenechea, B., Mitchell, J. A., Lopes, S., Reik, W. et al. (2004). Active genes dynamically colocalize to shared sites of ongoing transcription. *Nat. Genet.* **36**, 1065-1071.

Ottaviani, A., Schluth-Bolard, C., Rival-Gervier, S., Boussouar, A., Rondier, D., Foerster, A. M., Morere, J., Bauwens, S., Gazzo, S., Callet-Bauchu, E. et al. (2009). Identification of a perinuclear positioning element in human subtelomeres that requires A-type lamins and CTCF. *EMBO J.* **28**, 2428-2436.

Parada, L. and Misteli, T. (2002). Chromosome positioning in the interphase nucleus. *Trends Cell Biol.* **12**, 425-432.

Parada, L. A., McQueen, P. G., Munson, P. J. and Misteli, T. (2002). Conservation of relative chromosome positioning in normal and cancer cells. *Curr. Biol.* **12**, 1692-1697.

Parada, L. A., McQueen, P. G. and Misteli, T. (2004). Tissue-specific spatial organization of genomes. *Genome Biol.* **5**, R44.

Pierron, G. and Puvion-Dutilleul, F. (1999). An anchorage nuclear structure for telomeric DNA repeats in HeLa cells. *Chromosome Res.* **7**, 581-592.

Puri, M. and Sen, P. (1971). *Nonparametric Methods in Multivariate Analysis.* John Wiley and Sons.

Rouquette, J., Cremer, C., Cremer, T. and Fakan, S. (2010). Functional nuclear architecture studied by microscopy: present and future. *Int. Rev. Cell Mol. Biol.* **282**, 1-90.

Sabatier, L., Ricoul, M., Pottier, G. and Murnane, J. P. (2005). The loss of a single telomere can result in instability of multiple chromosomes in a human tumor cell line. *Mol. Cancer Res.* **3**, 139-150.

Scheuermann, M. O., Tajbakhsh, J., Kurz, A., Saracoglu, K., Eils, R. and Lichter, P. (2004). Topology of genes and nontranscribed sequences in human interphase nuclei. *Exp. Cell Res.* **301**, 266-279.

Shopland, L. S., Lynch, C. R., Peterson, K. A., Thornton, K., Kepper, N., Hase, J., Stein, S., Vincent, S., Molloy, K. R., Kreth, G. et al. (2006). Folding and organization of a contiguous chromosome region according to the gene distribution pattern in primary genomic sequence. *J. Cell Biol.* **174**, 27-38.

Solovei, I., Cavallo, A., Schermelleh, L., Jaunin, F., Scasselati, C., Cmarko, D., Cremer, C., Fakan, S. and Cremer, T. (2002). Spatial preservation of nuclear chromatin architecture during three-dimensional fluorescence in situ hybridization (3D-FISH). *Exp. Cell Res.* **276**, 10-23.

Solovei, I., Kreysing, M., Lanctot, C., Kosem, S., Peichl, L., Cremer, T., Guck, J. and Joffe, B. (2009). Nuclear architecture of rod photoreceptor cells adapts to vision in mammalian evolution. *Cell* **137**, 356-368.

Sun, H. B., Shen, J. and Yokota, H. (2000). Size-dependent positioning of human chromosomes in interphase nuclei. *Biophys. J.* **79**, 184-190.

Tanabe, H., Muller, S., Neusser, M., von Hase, J., Calcagno, E., Cremer, M., Solovei, I., Cremer, C. and Cremer, T. (2002). Evolutionary conservation of chromosome territory arrangements in cell nuclei from higher primates. *Proc. Natl. Acad. Sci. USA* **99**, 4424-4429.

Tanabe, H., Kupper, K., Ishida, T., Neusser, M. and Mizusawa, H. (2005). Inter- and intra-specific gene-density-correlated radial chromosome territory arrangements are conserved in Old World monkeys. *Cytogenet. Genome Res.* **108**, 255-261.

Teller, K., Solovei, I., Buiting, K., Horsthemke, B. and Cremer, T. (2007). Maintenance of imprinting and nuclear architecture in cycling cells. *Proc. Natl. Acad. Sci. USA* **104**, 14970-14975.

Weipoltshammer, K., Schofer, C., Almeder, M., Philimonenko, V. V., Frei, K., Wachtler, F. and Hozak, P. (1999). Intranuclear anchoring of repetitive DNA sequences: centromeres, telomeres, and ribosomal DNA. *J. Cell Biol.* **147**, 1409-1418.

Xu, N., Tsai, C. L. and Lee, J. T. (2006). Transient homologous chromosome pairing marks the onset of X inactivation. *Science* **311**, 1149-1152.

Zink, D., Amaral, M. D., Englmann, A., Lang, S., Clarke, L. A., Rudolph, C., Alt, F., Luther, K., Braz, C., Sadoni, N. et al. (2004). Transcription-dependent spatial arrangements of CFTR and adjacent genes in human cell nuclei. *J. Cell Biol.* **166**, 815-825.

Zinner, R., Teller, K., Versteeg, R., Cremer, T. and Cremer, M. (2007). Biochemistry meets nuclear architecture: multicolor immuno-FISH for co-localization analysis of chromosome segments and differentially expressed gene loci with various histone methylations. *Adv. Enzyme Regul.* **47**, 223-241.